Atmospheric Environment 140 (2016) 202–212

Contents lists available at ScienceDirect

Atmospheric Environment

journal homepage: www.elsevier.com/locate/atmosenv

All-optical automatic pollen identification: Towards an operational system

Benoît Crouzy*, Michelle Stella, Thomas Konzelmann, Bertrand Calpini, Bernard Clot

Federal Office of Meteorology and Climatology MeteoSwiss, Chemin de l'Aérologie, CH-1530 Payerne, Switzerland

HIGHLIGHTS

- We present results of a monitoring campaign using an optical pollen detector.
- We propose criteria for the evaluation of automatic pollen monitoring devices.
- The detector is able to discriminate between different pollen taxa.
- We can monitor in real time the total pollen and the grass pollen concentration.
- Due to the high sampling, we obtain statistically significant hourly concentrations.

ARTICLE INFO

Article history:
Received 28 January 2016
Received in revised form
30 May 2016
Accepted 31 May 2016
Available online 2 June 2016

Keywords:
Pollen
Automatic monitoring
Optical methods
Real-time
Supervised learning

ABSTRACT

We present results from the development and validation campaign of an optical pollen monitoring method based on time-resolved scattering and fluorescence. Focus is first set on supervised learning algorithms for pollen-taxa identification and on the determination of aerosol properties (particle size and shape). The identification capability provides a basis for a pre-operational automatic pollen season monitoring performed in parallel to manual reference measurements (Hirst-type volumetric samplers). Airborne concentrations obtained from the automatic system are compatible with those from the manual method regarding total pollen and the automatic device provides real-time data reliably (one week interruption over five months). In addition, although the calibration dataset still needs to be completed, we are able to follow the grass pollen season. The high sampling from the automatic device allows to go beyond the commonly-presented daily values and we obtain statistically significant hourly concentrations. Finally, we discuss remaining challenges for obtaining an operational automatic monitoring system and how the generic validation environment developed for the present campaign could be used for further tests of automatic pollen monitoring devices.

1. Introduction

The explosion of the prevalence of pollinosis over the last decades (Greiner et al., 2012; Wüthrich et al., 1995), which has reached 20% in many developed countries, has led to an intensive research activity and has contributed to the affirmation of aerobiology as an independent discipline. Monitoring airborne pollen concentration is of crucial importance in a context of dramatic anthropogenic changes influencing the airborne pollen quantity, spectrum and quality (Beggs, 2004; Ziska et al., 2011). Particularly important amongst human-driven factors relevant for pollen are climate change, urbanization and pollutant emission (D'Amato et al., 2001, 2007; Ring et al., 2001). Pollen concentrations provided by aerobiological networks are conveyed to various users, with different and sometimes contradictory needs. On one hand phenologists are principally concerned with continuous data series in order to be able to sort out significant trends in the plant annual rhythms, while on the other hand allergologists, pharmaceutical companies and patients principally need timely information on exposure levels. From the point of view of particle-transport numerical modeling, real-time data as input is a crucial factor for running precise simulations (Chamecki et al., 2009), which has led to the use of emission models in the absence of such data (Sofiev et al., 2006; Vogel et al., 2008; Zink et al., 2013; Pauling et al., 2012).

Traditionally, the pollen concentration is determined by Hirst-type volumetric samplers (Hirst, 1952): particles impact on a

* Corresponding author.
E-mail address: crouzy@gmail.com (B. Crouzy).

http://dx.doi.org/10.1016/j.atmosenv.2016.05.062

rotating tape and pollen and spores are identified by human operators using optical microscopy. The sturdiness of Hirst-type particle samplers has led to their adoption by various international aerobiological networks and efforts are being made towards standardization (Galán et al., 2014) and quality control (Oteros et al., 2013) in order to ensure continuity and comparability of time series. However, the strong dependence on (typically limited) human resources imposes trade-offs between spatial and temporal resolution. It is unfeasible to read complete tapes for a dense spatial coverage of a territory: the pollen concentration provided by aerobiological networks is thus usually not statistically significant below a daily time resolution, although bi-hourly values are sometimes presented (Comtois et al., 1999). Note that we do not refer here to the identification error, which is typically small as confirmed by so-called ring tests (Galán et al., 2014; Cotos-Yáñez et al., 2013). Coverage is also limited to a very small number of representative regions within countries. In addition, the tapes are usually changed for analysis once a week, leading to a delay between particle collection and diffusion of the information.

Motivated by users' demand for real-time pollen data, automatic monitoring systems have been tested over the last few years. The variety of systems reflects the compromises that need to be made with regards to an ideal automatic system. In this paper we propose the following four criteria for the evaluation of an automatic pollen monitoring device. The ability to *function reliably (1)* with minimal human intervention comes probably first. *Identifying (2)* and *counting (3)* different bioaerosols are two related but not equivalent tasks critical for evaluating a system. Together with counting come questions on the statistical significance of the sampling and its isokineticity. Finally, the ability for a system to *identify and count other aerosols than pollen (4)* could be critical in justifying investments for an automatic network: costs could be shared between different aerosol monitoring networks.

Amongst the proposed candidates which have approached or reached operational level, one can roughly distinguish between devices based on automatic image recognition such as the Hund BAA500 (Oteros et al., 2015) and systems based on air-flow cytometry such as the Yamatronics KH-3000 (Kawashima et al., 2007) or the WIBS sensor (for a recent study performed with the WIBS, see for example Perring et al. (2015)). In order to distinguish biological particles from other aerosols, optical detectors typically make use of the fluorescence of bioparticles (O'Connor et al., 2011). The different systems score differently well regarding the four criteria introduced above. Unsurprisingly, simplicity is often associated with high reliability and good sampling but modest identification capabilities.

In this paper, we focus on an air-flow cytometer, the Plair PA-300 (Kiselev et al., 2011, 2013), currently in validation phase at the Federal Office of Meteorology and Climatology MeteoSwiss (denoted "MeteoSwiss" hereafter). We present the results of the 2015 calibration and validation campaign at the light of the criteria from the list proposed above. The capabilities of the Plair PA-300 for measurements on aerosols within the range $10 - 100$ μm were tested, although the device could have a potential for the detection of spores, particulate matter and bacteria. The principal task of the present campaign was to link light scattering and fluorescence data with the morphology and composition of pollen grains. Accordingly, with reference to the criteria introduced earlier, we focused on the *identification* of pollen types in order to prepare the following monitoring campaign and approach operational level. The results, allowed to go beyond the mere identification task and we could already follow to a good extent the pollen season of individual pollen taxa.

2. Material and methods

2.1. Study site

Calibrations and season monitoring were performed on the roof of the MeteoSwiss two-storey building (building height 7 m, ground altitude 490 m and WGS84 coordinates 46°48′48″ N, 6°56′35″ E), located in a rural environment close to Payerne, Switzerland (Fig. 1). The presence of two volumetric Hirst-type pollen traps operating in parallel on the site provided a reference for evaluating the results of the automatic device. One detector was used for reference and the other as backup in case of missing data. The choice of Payerne for running the campaign was motivated by the fact that various pollen types can be measured in Payerne and the combinations of pollens observed are typical for what can be found on the Swiss Plateau, by far the most populated region of Switzerland (home of over two-thirds of the Swiss population). These factors make Payerne a good site for testing and developing new devices.

2.2. Description of the optical device

We used the first unit of the commercially-available PA-300 detector produced by Plair SA in Geneva (see Fig. 2). Although we recall here some general features of the device, a comprehensive technical description can be found elsewhere (Kiselev et al., 2011, 2013). Particles first pass through a red laser beam (658 nm) and time-resolved scattering data is recorded by two photo-detectors. The scattering signal helps to characterize the optical size, the shape and the surface properties of the particles. A second laser beam in the UV range (337 nm) excites the particles and the wavelength-resolved fluorescence signal is recorded using diffraction grating and an array of 32 photo-detectors (32 equal bins with overall range 390–600 nm). In addition, the phosphorescence (long-time response) is recorded by the two photo-detectors used for the scattering signal and the short-time response by an ultrafast photo-detector. For a summary on the time resolution and the wavelength detection range of the different detectors, see Table 1.

2.3. Description of the inlet system

Air was pumped into the detector at a flow rate of 2 l/min. In order to increase aerosol sampling, a concentrator based on virtual impactor principle was used with the instrument. The concentrator was provided by Plair SA as an option to the PA-300. The major air outlet of the concentrator was connected to the second pump (flow rate 30 l/min) and the minor outlet to the device. Finally, a Sigma-2 inlet (Verein Deutscher Ingenieure, 2013) was put on top of the concentrator for particle sampling and protection of the detector from the rain (see panels A and C of Fig. 1).

2.4. Manual reference counts

As reference for the automatic counts, we used the current standard method in aerobiological networks (Galán et al., 2014; Hirst, 1952). Hirst-type volumetric samplers (we used a detector from Burkard Scientific Ltd.) collect airborne particles on a rotating drum (efficient impaction for particle size larger than 5 μm). Counting of pollen grains was performed at MeteoSwiss using the same procedure as for the operational monitoring of the pollen season (optical microscope Olympus BX45 magnification 600x). Results are summarized in tables with average daily concentration of 47 pollen types plus one category for unidentified pollen. As for operational pollen measurements, counting all the grains present on the tape was not feasible due to the duration of the pollen

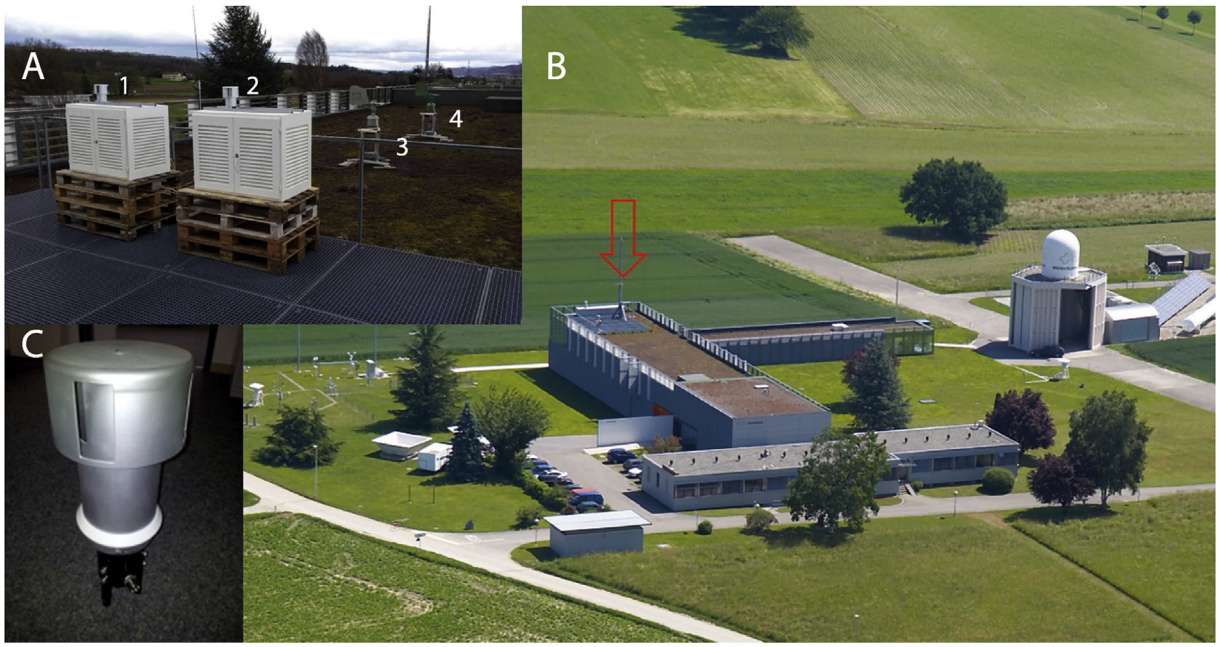

Fig. 1. Validation setup with boxes for automatic detectors (panel A, 1 and 2) and volumetric Hirst-type samplers (panel A, 3 and 4); MeteoSwiss study site in Payerne, Switzerland (panel B); Details of the Sigma-2 inlet used for the automatic device (panel C).

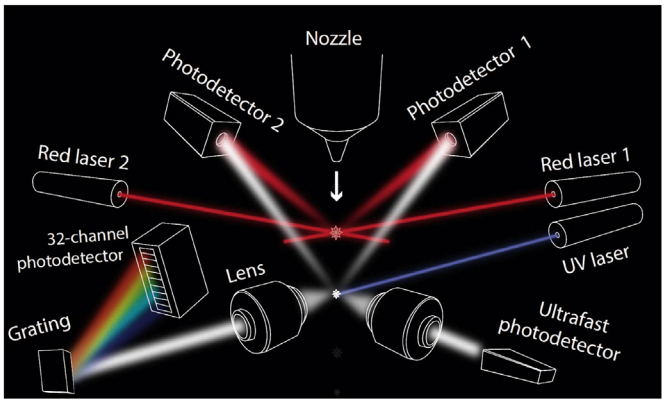

Fig. 2. Schematics of the Plair PA-300 detector (courtesy of Plair S.A.).

campaign between pollen concentrations from three Hirst samplers running in parallel yield an average relative fluctuation over the season of around 30%. The reference Hirst device suffered two failures, resulting in the loss of fourteen days of data. Out of those missing days, twelve could be replaced using data from the Hirst sampler running in parallel.

2.5. Data processing and network interface

Scattering and fluorescence optical data was recorded by the onboard computer of the detector, which in turn could be accessed via FTP. Preprocessing of the complete time-resolved scattering signal reduced it to 18 features. The complete list of optical features of the measured events can be found in Table 1. In order to classify particles we based us on those features and developed a calibration library.

Table 1
Summary of the optical data produced by the Plair PA-300 detector. With reference to Fig. 2 two scattering signals are recorded: for laser 1 the signals from photodetector 2 and 1 are denoted primary and secondary scattering trace respectively (and conversely for laser 2).

Optical parameter	Features number	Description
Fluorescence	32 bins	Fluorescence intensity between 390 and 600 nm
Primary scattering trace	14	Both photodetectors: trace integral below and above half of the maximum; trace duration and maximum; timing of maximum; number of local extrema (min and max)
Secondary scattering trace	4	Both photodetectors: Trace integral and maximum
Fast decay of fluorescence	8 bins	Fluorescence after {4,8,16,32,64,128,256} ns and saturation time in ns.
Phosphorescence	8 bins	Phosphorescence between 650–700 nm and between 650–850 nm after {1.6,3.2,6.4,12.8} μs

campaign (two longitudinal lines were counted). Two Hirst samplers were run in parallel in order to ensure completeness of reference data throughout the season (See Fig. 1). As a result of the limited surface examined, reference concentrations could not practically be used below the time resolution of one day. For the total pollen concentration, the comparison over a preceding

2.6. Calibration pollen

Fresh pollen samples were collected manually for six different taxa while for twelve others dried pollen was bought (supplier: Bonapol A.S., Czech Republic). Dry pollen was used to test on a larger range the ability of the Plair device to recognize physical

features of pollen grains and, as the real state of pollen (fresh/dry or respectively swollen/deflated) in the air is not well known, to test the ability of the PA-300 to identify particles that could possibly present such differences. A summary of the calibration material can be found in Table 2. For each pollen type, a subsample was fixed on a slide and examined in order to check the state of the pollen grains and the sample purity. We checked the plausibility of the tabulated values for the size of all the pollen samples by microscope inspection for both fresh pollen and non re-hydrated dry pollen. Pollen was released 50 cm upwind of the measuring device inlet and the recorded events were used to train the classification algorithm and to evaluate the performance of the classification. The resulting number of calibration optical events is summarized in Table 1. We used 80% of the dataset for training supervised learning algorithms and 20% for evaluating the performance of the classifiers. The number of events varied significantly when considering different taxa due to uneven sample quality: for some taxa aggregation of the grains was observed, resulting in a more difficult insertion in the monitoring device. In this regard, fresh pollen could be most easily handled. In addition, we put more effort in obtaining a sufficient calibration dataset for the main allergenic taxa present in Payerne (birch, hazel, ash and grass pollen).

2.7. Particle size and morphology

To compute particle size, we made the (crude) approximation of geometric light scattering by spheres and used the fact that under this approximation scattering amplitudes are expected to be proportional to the square of the particle radius. The proportionality constant was estimated using 16 known pollen types (see Section 3.1). Relevant for the optical-size estimation were both the primary and the secondary scattering traces (four traces in total, see Table 1) and we took the maximum between the computed optical sizes. Note that while for the two primary traces the whole scattering signal could be used for the scattering-amplitude estimation, only the maxima of the two secondary traces was significant (lower signal-to-noise ratio). The expected average size was obtained from the literature (Beug, 2004) and checked by direct inspection under a microscope.

Regarding particle morphology, we made use of the number of local maxima of the scattering signal (Mie, 1908) and of its "peakedness" P, which we estimated as the ratio between the integral of the signal above half of the maximal signal amplitude and the total signal integral

$$P = \frac{\int_{t_{1/2}^1}^{t_{1/2}^2} I(t)\mathrm{d}t}{\int_{-\infty}^{\infty} I(t)\mathrm{d}t}, \quad (1)$$

with I(t) the amplitude of the scattering signal at a time t and $t_{1/2}^{1,2}$ the closest times (compared to the time t_{max} when the scattering amplitude is maximal) satisfying $I(t_{1/2}^{1,2}) = I_{max}/2$. The peakedness quantifies how sharp the peak distribution is.

Table 2
Summary of the taxa used for calibration. The label "n.a." refers to taxa for which a very large number of plants was used for collecting the pollen sample and the label "unknown" to the number of trees used for collection by the pollen supplier.

Species	State	Number of plants	Calibration events
Alnus glutinosa	Dry	unknown	2063
Ambrosia artemisiifolia	Dry	n.a.	870
Artemisia vulgaris	Dry	n.a.	2375
Betula pendula	Fresh	3	7560
Carpinus betulus	Fresh	1	3610
Castanea sativa	Dry	unknown	1268
Cedrus sp.	Dry	unknown	853
Corylus avellana	Fresh	1	3013
Dactylis glomerata	Fresh	n.a.	4132
Fagus sylvatica	Dry	unknown	1950
Fraxinus excelsior	Dry	unknown	4091
Helianthus annuus	Dry	unknown	496
Olea europaea	Dry	unknown	1980
Phleum pratense	Dry	n.a.	2244
Plantago lanceolata	Fresh	n.a.	1271
Platanus × *acerifolia*	Dry	unknown	3207
Quercus robur	Fresh	1	3531
Zea mays	Dry	n.a.	800

2.8. Particle classification

In order to quantify the performance of classification algorithms we used two metrics: precision and recall (Blair, 1979). Precision is given by the fraction of retrieved instances that are relevant and recall by the fraction of relevant instances that are retrieved. No further metrics (F-measure, for example) seemed necessary for our purposes since we obtained very close values for precision and recall.

Support vector machine algorithms (denoted "SVM" hereafter) are at the core of our classification of optical events. Those supervised-learning algorithms are based on computing optimal hyperplanes separating data into classes within the feature space. The separation is optimal in the sense that the plane resulting in the largest margin is computed. In the event when the calibration data is not separable by hyperplanes, non-linear transformations of the feature space can be introduced (which is usually colloquially referred to as "Kernel trick") in order to obtain a linearly-separable classification problem. A further important concept is the idea of soft-margin SVMs which allow to account for the presence of mislabeled data through a penalty. We shall not present a detailed review on SVMs here and simply refer to Vapnik (1998) for more details. Specifically, we used LIBSVM (Chang and Lin, 2011) as implementation of the soft-margin SVM classification algorithms and worked with the standard RBF Kernel. Kernel parameters and parameters accounting for mislabels were optimized regarding the precision and recall metrics using a simple grid search. LIBSVM provides in addition to the classification an estimation of its reliability for given data-points according to their position in the feature space. Specifically, this estimation bases on the distance of the events (characterized by the optical parameters) from the maximal-margin hyperplane of their respective class (Platt, 1999; Chang and Lin, 2011). We used this technique to reduce the number of false positive (albeit at the expense of sampling) when following the pollen season of individual taxa.

As alternative, artificial neural networks "ANN" hereafter) are also frequently used for supervised learning classification, although they require more caution than SVMs in order to avoid overtraining (Tetko et al., 1995). Elements of the feature vectors are used as weighed inputs triggering the response of neurons organized in layers, the response of neurons being used as inputs for the neurons of the subsequent layer. Training of the network consists in optimizing the weights given to the different inputs in order to correctly classify the largest proportion of data. Finally, the intensity of the response of the neurons of the final layer relates to the degree of likelihood of a given label (voting system). Introducing a cutoff for the response intensity, one may as for the SVM reduce the number of false positive in the classification at the expense of sampling. Specifically, we trained a neural network (Venables and Ripley, 2002) with one hidden layer and found that best performance was achieved using 11 hidden nodes (additional

nodes led to over-training). The output of neurons was determined by a softmax function (Sutton and Barto, 1998)

$$O_j = \frac{e^{\mathbf{w}_j \cdot \mathbf{x}}}{\sum_i e^{\mathbf{w}_i \cdot \mathbf{x}}}, \quad (2)$$

with j the neuron index within the layer, $\mathbf{w}_j$ the vector containing the weights given to the different inputs (different for each neurons) and $\mathbf{x}$ a vector containing the outputs of the preceding layer.

For following the grass pollen season we introduced a heterogeneous classifier (Zhou, 2012) based on the combination of the ANN and the SVM. Precision could be increased by keeping only the labels for which the ANN and the SVM gave the same prediction and taking advantage of the different bias of the two methods.

3. Results

3.1. Size and morphology

In order to classify data it is crucial to use as much a-priori information as possible. This is especially true since SVMs operate in a modified feature space, which makes the interpretation of results difficult. Size, morphology and composition of the pollen grain are in this regard obvious features which need to be coherently measured.

Measuring the grain size first allowed to test the reliability of the optical measurements. Secondly, although the pollen grains of a given species present a large variability, determining their size already limits the number of possible labels prior to applying more elaborate classification algorithms. In Fig. 3 we present a comparison between measured size and expected average size for 16 pollen types. Note that the two largest pollen types (*Cedrus* sp. and *Zea mays*) are not present in this figure: examination of the two dried samples under the microscope showed significant collapse of the grains precluding their use as reference. *Helianthus annuus* pollen grains initially presented on average a significantly smaller size than in the literature. After inspection of the sample under the optical microscope, the deviation could be ascribed to the presence of large spikes and the measured average value (disregarding spikes) was used instead of the tabulated grain size for *Helianthus annuus* pollen (that includes the spikes). For the 15 other pollen taxa the average size value from tables (Beug, 2004) was used. The optical measurements correlated well with the expected values ($R^2 = 0.88$). Considering the large intrinsic variability of the grain size (Beug, 2004), the dependence of the size on the conditions (fresh/dry), the possible presence of aggregates and the strong deviations from the ideal-sphere approximation made for estimating the optical size, the differences between expected and measured size appear reasonable.

Second-order features (sharpness of the peak scattering amplitude, denoted "peakedness" and presence of local extrema) of the time-resolved scattering signal gave us additional insight into the morphology of the pollen grains. While the size could be estimated straightforwardly from the scattering amplitudes, the interpretation of second-order features was trickier since they are the result of combined factors such as particle shape and size or the presence of irregularities at the surface of the grains. In Fig. 4 we present the average values of two features of the scattering signal: peakedness (see Equation (1)) and number of local maxima. While both features correlate with the size, deviations from the size ordering due to the grain shape and/or surface irregularities gave a further degree of discrimination between different taxa.

3.2. Fluorescence spectrum

Fluorescence is essential for distinguishing biological particles from other aerosols. In Fig. 5 we present the scaled fluorescence spectra of the 18 pollen types used for calibration. The average spectra present some similarities. It is thus clear that the spectrum is not always sufficient for conclusively discriminating between pollen taxa. Fluorescence can however be used to identify pollen

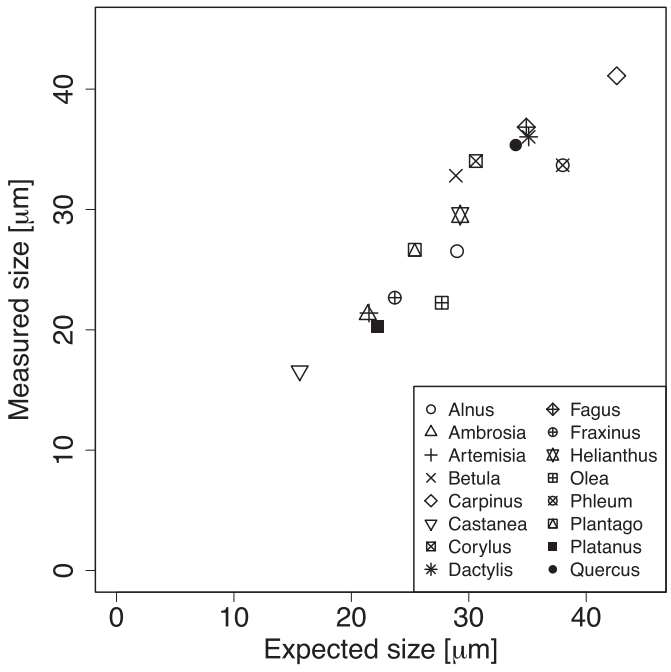

Fig. 3. Comparison between tabulated and measured average size of pollen grains ($R^2 = 0.88$) with a cutoff at 60 µm in optical measurements to filter out aggregated pollen grains (calibration dataset described in Table 2).

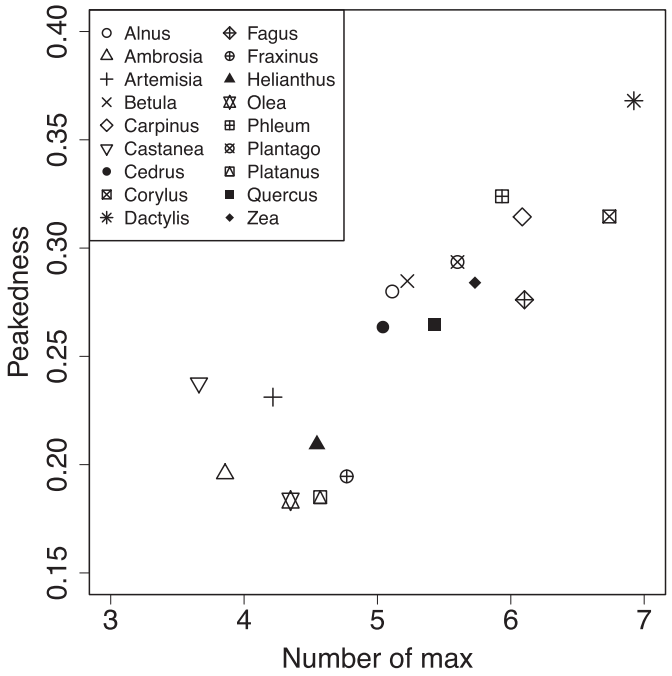

Fig. 4. Average peakedness (as defined in Equation (1)) of the time-resolved scattering amplitude versus average number of local maxima (calibration dataset described in Table 2).

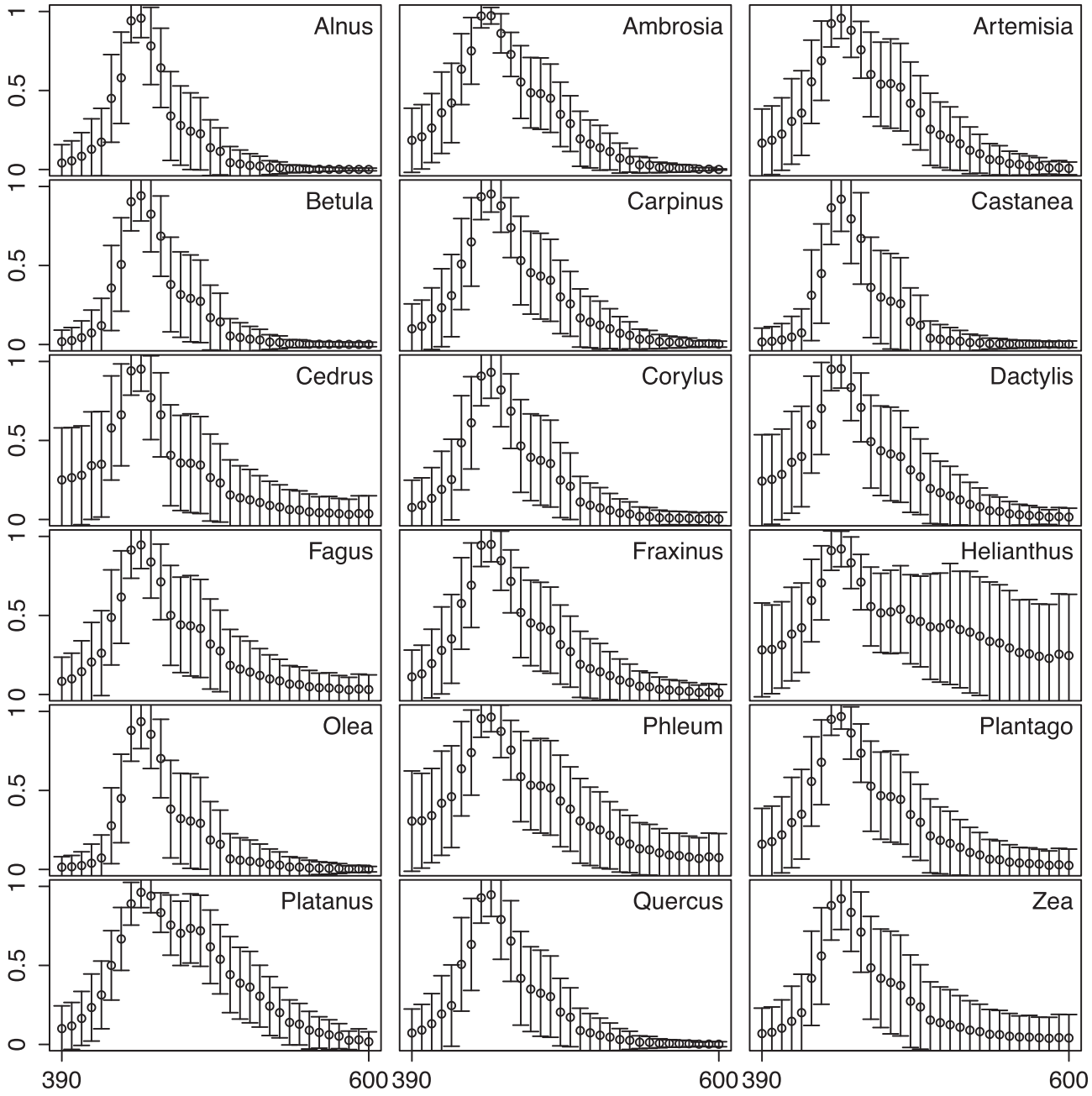

Fig. 5. Average and standard deviation of the fluorescence spectrum for the 18 taxa of the calibration dataset (see Table 2). All spectra were scaled to one using the maximal fluorescence amplitude. The bars indicate plus or minus one standard deviation on the average spectrum.

and differences in the spectra allow, in certain situations, to exclude some labels. For example, the measurement of a non-zero fluorescence amplitude around 600 nm is incompatible with a pollen from the Betulaceae family (*Alnus*, *Carpinus*, *Corylus* and *Betula*) but could possibly be observed for grass pollen (*Dactylis* and *Phleum*).

3.3. Pollen identification: calibration

The first step in calibrating the device for pollen-taxa identification consisted in using the recorded scattering and fluorescence events for the known pollen types in order to train the SVM or the ANN. Before performing this calibration, we checked whether the optical signals and event statistics could be considered independent of the conditions by inserting the same pollen under different humidity and temperature conditions. While most optical parameters remained stable, four parameters presented a significant change (phosphorescence intensity between 650 and 850 nm, see Table 1). Those parameters were thus excluded from the analysis in order to avoid artificial classification performance unrelated to the actual differences between the pollen grains. In other words, using those features we would have trained the SVM or the ANN to recognize the conditions of the experiments instead of the intrinsic optical properties of the pollen grains. This would in turn have resulted in poor performance when comparing the automatic measurements to the reference manual measurements.

The results of the classifications performed with the ANN are presented in Table 3. Note that those classifications were performed considering only the fresh pollen taxa (mostly relevant for

Table 3
Confusion table for pollen taxa identification by the ANN algorithm. The bold values in the bottom right represent the average precision 82% and recall 81%.

	Betu.	Carp.	Cory.	Dact.	Frax.	Plan.	Plat.	Quer.	**Recall**	
Betu.	**985**	54	7	33	28	6	1	70	0.83	
Carp.	135	**452**	0	43	6	4	0	11	0.69	
Cory.	6	0	**480**	3	8	4	0	11	0.94	
Dact.	65	29	4	**530**	57	12	1	30	0.73	
Frax.	35	6	7	30	**621**	8	3	36	0.83	
Plan.	6	7	7	4	12	**170**	21	6	0.73	
Plat.	1	0	1	0	3	8	**620**	0	0.98	
Quer.	79	4	13	22	41	1	1	**423**	0.72	
Precision	0.75	0.82	0.92	0.80	0.80	0.80	0.96	0.72		**0.82**
									0.81	

following the actual pollen season) and the two dry pollen taxa with the most optical events from our calibration dataset. For the SVM classifier (Table 4), on average, the same precision and recall as for the ANN were obtained, although for individual taxa precision and recall values differed by up to 6%. For both classifiers it was possible to select the most certain predictions. Table 5 presents the results of the classification after selection of the 78% of the events located the furthest from the boundary of clusters in the data space. Removing 22% of the events allowed to gain 9% precision on average. A narrower selection criterion further increases precision, albeit at the expense of sampling. Similar results (correct taxum identification for more than 90% of the events considered) could be obtained when selecting the events after ANN classification according to the value of the output of the final-layer neurons (not shown).

3.4. Comparison with manual measurements

A good insight into the identification capabilities of the Plair PA-300 was obtained from the results of the previous Section. However, a device candidate for operational use can only be fully tested by conducing an in-situ operational season monitoring (14th of February - 31st of August). Presenting a limited number of particles with a good purity grade remains indeed to a good extent an academic task. Over a season, pollen grains from the same species are measured by the detector under a variety of temperature and humidity conditions. In addition, the vast majority of aerosols needs to be disregarded (Pöschl, 2005) for being either non biological (e.g. particulate matter) or unrelated to pollen (e.g. spores and bacteria). Of crucial importance is also testing throughout the season the distinction between the typical combinations of pollens present in the air simultaneously.

Monitoring the total pollen concentration was a suitable benchmark for our ability to exclude the above-mentioned irrelevant particles and for the representativity of the sampling. Besides the advantage of allowing to avoid concurrent taxum-identification errors and sampling errors, working with the total pollen concentrations provided reference measurements with more representative sampling than the sampling of individual taxa. In order to identify airborne pollen grains disregarding the taxum, the simple approach of counting all the events fluorescing between 390 and 600 nm was used. This criterion already provided good results that could be improved by introducing cutoffs (compatibility with pollen) for the optical size at 9 μm and for the fluorescence intensity. Those two thresholds were determined making a trade-off between precision (determined a-posteriori from comparison with manual measurements) and sampling. The results of the comparison between automatic and manual measurements are presented in Fig. 6.

Due to the presence of the virtual impactor and associated possible particle loss, it was difficult to estimate the volume actually sampled by the Plair detector. Scaling the curves to recover the same annual total pollen sum as in manual measurements, we obtained that sampling with the Plair PA-300 was about 25 times higher than sampling from the manual counts. In other words, pollen concentration values from the automatic counts in Fig. 6 were based on 25 times more events than the pollen concentrations from the manual measurements. Considering the total volume sampled in the inlet of the automatic device (Sigma-2), one could have theoretically obtained a larger increase of the sampling

Table 4
Confusion table for pollen taxa identification by the SVM algorithm. The bold values in the bottom right represent the average precision 82% and recall 81%.

	Betu.	Carp.	Cory.	Dact.	Frax.	Plan.	Plat.	Quer.	**Recall**	
Betu.	**1018**	57	5	27	28	4	2	43	0.86	
Carp.	107	**478**	1	36	11	5	0	13	0.73	
Cory.	3	0	**482**	8	6	4	1	8	0.94	
Dact.	57	33	5	**535**	60	12	2	24	0.73	
Frax.	30	3	14	25	**635**	6	4	29	0.85	
Plan.	5	7	5	10	20	**157**	23	6	0.67	
Plat.	0	0	0	1	3	7	**622**	0	0.98	
Quer.	87	3	18	22	51	6	1	**396**	0.68	
Precision	0.78	0.82	0.91	0.81	0.78	0.78	0.95	0.76		**0.82**
									0.81	

Table 5
Confusion table for pollen taxa identification by the SVM algorithm after selection of the most reliable 78% of the events according to their position in the feature space. The bold values in the bottom right represent the average precision 91% and recall 89%.

	Betu.	Carp.	Cory.	Dact.	Frax.	Plan.	Plat.	Quer.	**Recall**	
Betu.	**849**	27	5	12	5	1	1	31	0.91	
Carp.	75	**422**	0	18	2	2	0	2	0.81	
Cory.	1	0	**466**	0	1	1	0	4	0.99	
Dact.	27	4	1	**439**	29	3	1	3	0.87	
Frax.	5	0	4	5	**525**	0	1	10	0.95	
Plan.	2	4	0	4	4	**98**	16	2	0.75	
Plat.	0	0	0	0	0	4	**606**	0	0.99	
Quer.	28	0	6	8	21	3	0	**304**	0.82	
Precision	0.86	0.92	0.97	0.90	0.89	0.88	0.97	0.85		**0.91**
									0.89	

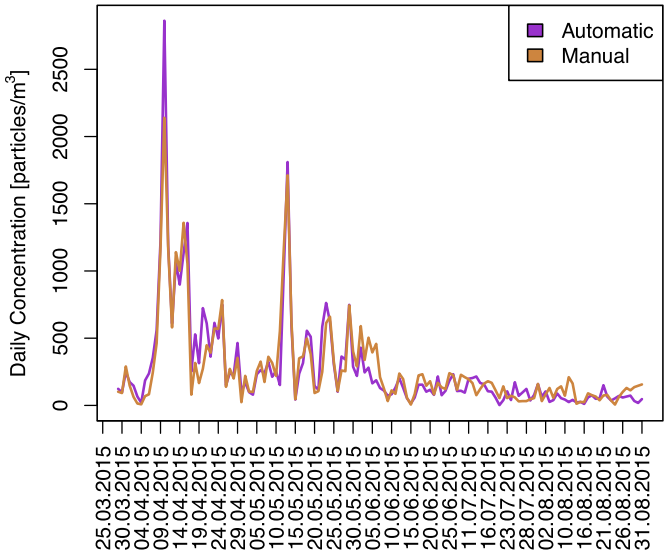

Fig. 6. Comparison between automatic (Plair PA-300) and manual (Hirst-type) total pollen counts. Pearson correlation coefficient $R = 0.95$.

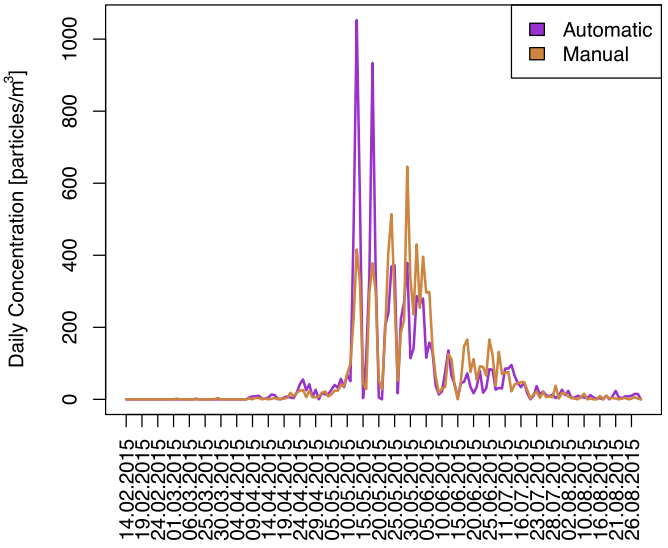

Fig. 7. Comparison between automatic (Plair PA-300) and manual (Hirst-type) grass pollen counts. Pearson correlation coefficient $R = 0.83$.

if no particle had been lost (3 times more air was sampled in the inlet of the Plair compared with the Hirst and in the Hirst only 3.5% of the band is read).

Using the classifiers (ANN and SVM) optimized by the calibration procedure described in the previous Section, we already tried to classify the pollen according to its fluorescence spectrum and the scattering signal. Note that the approach was intrinsically limited by the fact that only a small part of the pollen types present in the air was tested in calibrations. In addition, for most pollen types, we only had dried samples, which strongly differ from fresh pollen (more likely to be present in the air). The case of grass pollen already provided interesting results: using as a proxy for the Poaceae (grasses) the fresh *Dactylis glutinosa* sample and the dried *Phleum pratense* sample was sufficient for following to a good extent the grass pollen season (Fig. 7). In order to exploit the most of our calibration dataset, we combined the SVM and ANN classifiers and kept only the events considered as grass pollen by both methods. In addition, we introduced cutoffs in the prediction probability in order to exclude uncertain events. Best results were obtained with strict cutoffs, maintained until the beginning of the grass season which were relaxed as soon as significant non-zero grass pollen counts were observed.

4. Discussion

As mentioned in the Introduction, *reliability* is certainly the first criterion for evaluating an operational system. From the moment when the system with the final version of the inlet was installed (29th of March 2015) up to the end of the campaign (31th of August), the Plair PA-300 consistently delivered real-time data with only one interruption at the peak of a heat wave (1-9th of July) when we switched off the device for protecting it from possible damage (during the interruption the two-meter temperature typically reached 35°–38°). For comparison, recall that the Hirst volumetric sampler used for reference had 14 days of missing data due to issues with the internal clock of the device and for those 14 days data from the Hirst sampler running in parallel had to be used (when available). The issue with the heat shall be addressed using a cooling/heating unit during the next campaign and reliability will be further tested. In addition, maintaining a controlled operating temperature shall improve the stability of the optical signals.

The basic pollen *counting* ability could be estimated by the degree of correlation between the total pollen concentration obtained from the Plair device and the Hirst sampler. From the date of installation of the Sigma-2 inlet (29th of March) up to the end of the season (31st of August) we obtained a Pearson correlation of 0.95, a

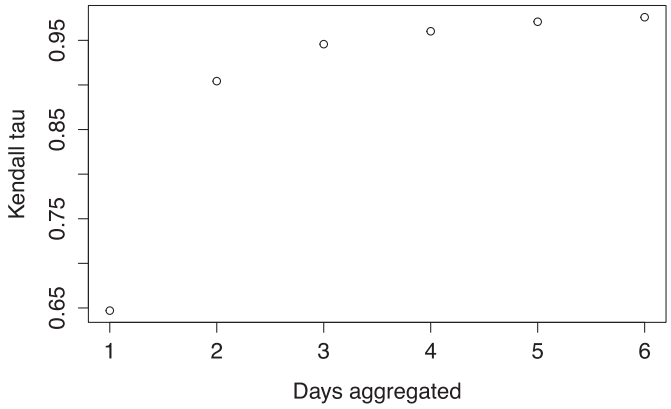

Fig. 8. Increase of Kendall rank correlation coefficient τ between aggregated automatic and manual counts as function of aggregating period.

Spearman rank correlation of 0.82 and a Kendall rank correlation coefficient τ of 0.65. For the beginning of the season without Sigma-2 the values of the coefficients were 0.58, 0.39 and 0.27, respectively. The high level of correlation between the two time series in the presence of the Sigma-2 confirmed the choice of this inlet solution. This convergence is remarkable considering the differences between the Sigma-2 inlet and the inlet of the Hirst, which might have resulted in different sampling rates depending on wind velocity and/or the type of particles. Part of the divergence between the manual and automatic signals can clearly be linked to sampling issues. In order to isolate it, the correlation between the signals from automatic and manual measurements was computed aggregating daily observations. As seen in Fig. 8, the Kendall rank correlation coefficient (the lowest correlation coefficient from our analysis) rapidly improves when aggregating data up to a plateau at around $\tau = 0.96$, suggesting that most of the observed deviation between the signals can be ascribed to the much lower sampling of manual measurements.

The higher sampling with the Plair PA-300 device allows to access a time resolution below the usual daily values from Hirst detectors. With a sampling 25 times better with the automatic system than with the Hirst, roughly the same degree of statistical significance is obtained with the Plair PA-300 at an hourly resolution as with the Hirst at a daily resolution. Airborne pollen concentration averaged over the day are not necessarily completely representative for exposure peaks (Clot, 2001; Puc, 2012; Bastl et al., 2016). In this regard, an automatic system could provide patients with information in real-time on actual exposure levels. In order to obtain meaningful values from manual measurements and compare hourly values from manual and automatic measurements, one needs to use average values (typically monthly averages). While no one-to-one comparison can be made for July (9 missing days in the automatic measurements), one can consider as examples the values of June and August that show similar daily profiles (Fig. 9), although noise is stronger for manual values.

Regarding the analysis on pollen morphology (particle size, shape and surface properties), the results confirmed the ability of the Plair PA-300 to capture those features. Beyond the interest for pollen taxa identification, this capability is promising for using the Plair PA-300 to identify and *count other aerosols than pollen* (biological or non-biological). As mentioned in the Introduction this could represent a serious advantage compared to systems allowing pollen identification only.

Although preliminary results were obtained, the investigations regarding the ability of the Plair PA-300 to *identify* different pollen types remain incomplete. Using dried pollen samples bought from a supplier had the advantage of standardization and control of sample purity. The use of libraries calibrated with dried pollen is however very limited for an operational pollen monitoring due to

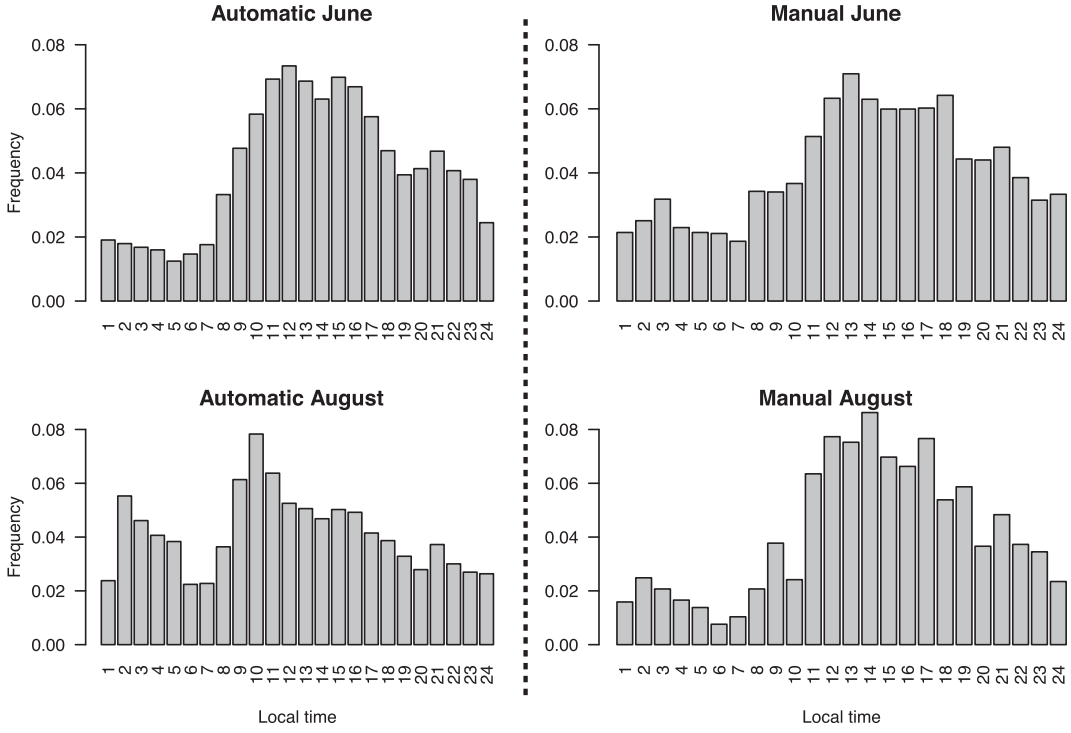

Fig. 9. Comparison between automatic (Plair PA-300) and manual (Hirst-type) average hourly values of total pollen concentration.

the morphological differences between fresh and dried pollen. We expect that best results can be obtained with samples inserted into the detector shortly after collection (within few hours). A systematic collection of fresh pollen samples is in this line planned for the next campaign. Considering that the state of pollen in the air (fresh/swollen or dry/deflated) is not well known and possibly varying, it is interesting to see that the PA-300 can correctly classify a large number of grains disregarding the state. Variability of the optical signals is currently the greatest limitation of the approach when trying to discriminate between pollen taxa. Considering the calibration dataset, we barely obtained individual differences between the parameter average values taken over two different taxa exceeding one standard deviation. This required going beyond traditional approaches like principal component analysis and use SVMs and ANNs.

5. Conclusion

Results of a pollen monitoring campaign were presented. We proceeded step by step in order to systematically investigate the potential of the Plair PA-300 for operational use in a pollen monitoring network. Statistical investigations on the optical data produced by the instrument were the natural first step. Those investigations provided a basis for aerosol identification using the Plair PA-300. We then performed calibrations inserting pollen manually into the device. Although controlled calibrations are essential, the real benchmark for the capabilities of the device is the pre-operational test performed comparing the results from automatic and manual monitoring. Resulting from this test is not only that the automatic system provides values that are in good agreement with manual reference values but also that the increased sampling makes real-time pollen monitoring possible.

The specificity of traditional pollen detectors may have limited the expansion of networks and the resources allocated to them. In this regard, a general-purpose particle detector, even if its pollen-identification ability remains imperfect, might allow to share investment costs between pollutants monitoring networks and biometeorological networks. In turn this could justify the existence of denser networks. The Plair PA-300 provides the end-user with raw optical data, which leaves a great deal of flexibility for calibrating the device in order to recognize various particles. Depending on user's needs, existing calibration libraries could be used in the future or custom algorithms developed with focus on the particles of interest.

Real-time data based on a statistically valid sample size opens new research directions in aerobiology and allergology. Accessing real exposure levels (beyond daily averages) could allow for better definitions on critical exposure thresholds statistically correlated to allergic symptoms. Patients would in turn access information on current exposure levels and take appropriate actions regarding their medications and the planning of activities. Concerning pollen forecasts, a real-time input could bring a significant increase in precision compared to the current weekly forecasts. In the same direction, numerical models for pollen transport would greatly benefit from inputs valid up to a timescale critical for determining the outcome of the simulations.

Acknowledgments

We thank Anne-Marie Rachoud for counting the reference pollen slides, Regula Gehrig for helpful discussions on uncertainties in manual pollen counts as well as for careful proofreading the manuscript and Jean-Marc Aellen for technical support. We are also grateful to Christian Félix for suggesting the use of the Sigma-2 as inlet.

References

O'Connor, D.J., Iacopino, D., Healy, D.A., O'Sullivan, D., Sodeau, J.R., 2011. The intrinsic fluorescence spectra of selected pollen and fungal spores. Atmos. Environ. 45 (35), 6451–6458. http://www.sciencedirect.com/science/article/pii/S1352231011007886.

Bastl, K., Kmenta, M., Pessi, A.-M., Prank, M., Saarto, A., Sofiev, M., Bergmann, K.-C., Buters, J.T., Thibaudon, M., Jäger, S., Berger, U., 2016. First comparison of symptom data with allergen content (Bet v. 1 and Phl p 5 measurements) and pollen data from four European regions during 2009–2011. Sci. Total Environ. 548–549, 229–235. http://www.sciencedirect.com/science/article/pii/S0048969716300134.

Beggs, P., 2004. Impacts of climate change on aeroallergens: past and future. Clin. Exp. Allergy 34 (10), 1507–1513.

Beug, H.-J., 2004. Leitfaden der Pollenbestimmung fur Mitteleuropa und angrenzende Gebiete. Verlag Friedrich Pfeil, Münich. ISBN 3 89937 043 0.

Blair, D.C., 1979. Information Retrieval. In: Van Rijsbergen, C.J. (Ed.), second ed. Butterworths, London, p. 208. http://dx.doi.org/10.1002/asi.4630300621. Journal of the American Society for Information Science 30(6), 374–375.

Chamecki, M., Meneveau, C., Parlange, M.B., 2009. Large eddy simulation of pollen transport in the atmospheric boundary layer. J. Aerosol Sci. 40 (3), 241–255.

Chang, C.-C., Lin, C.-J., 2011. LIBSVM: a library for support vector machines. ACM Trans. Intell. Syst. Technol. 2, 1–27 software available at: http://www.csie.ntu.edu.tw/cjlin/libsvm.

Clot, B., 2001. Airborne birch pollen in Neuchâtel (Switzerland): onset, peak and daily patterns. Aerobiologia 17 (1), 25–29. http://dx.doi.org/10.1023/A%3A1007652220568.

Comtois, P., Alcazar, P., Néron, D., 1999. Pollen counts statistics and its relevance to precision. Aerobiologia 15 (1), 19–28.

Cotos-Yáñez, T.R., Rodríguez-Rajo, F.J., Pérez-González, A., Aira, M.J., Jato, V., 2013. Quality control in Aerobiology: comparison different slide reading methods. Aerobiologia 29 (1), 1–11. http://dx.doi.org/10.1007/s10453-012-9263-1.

D'Amato, G., Liccardi, G., D'Amato, M., Cazzola, M., 2001. The role of outdoor air pollution and climatic changes on the rising trends in respiratory allergy. Respir. Med. 95 (7), 606–611. http://www.sciencedirect.com/science/article/pii/S0954611101911126.

D'Amato, G., Cecchi, L., Bonini, S., Nunes, C., Annesi-Maesano, I., Behrendt, H., Liccardi, G., Popov, T., Van Cauwenberge, P., 2007. Allergenic pollen and pollen allergy in Europe. Allergy 62 (9), 976–990. http://dx.doi.org/10.1111/j.1398-9995.2007.01393.x.

Galán, C., Smith, M., Thibaudon, M., Frenguelli, G., Oteros, J., Gehrig, R., Berger, U., Clot, B., Brandao, R., 2014. Pollen monitoring: minimum requirements and reproducibility of analysis. Aerobiologia 30 (4), 385–395.

Greiner, A.N., Hellings, P.W., Rotiroti, G., Scadding, G.K., 2012. Allergic rhinitis. Lancet 378 (9809), 2112–2122. http://www.sciencedirect.com/science/article/pii/S014067361160130X.

Hirst, J.M., 1952. An automatic volumetric spore trap. Ann. Appl. Biol. 39 (2), 257–265. http://dx.doi.org/10.1111/j.1744-7348.1952.tb00904.x.

Kawashima, S., Clot, B., Fujita, T., Takahashi, Y., Nakamura, K., 2007. An algorithm and a device for counting airborne pollen automatically using laser optics. Atmos. Environ. 41 (36), 7987–7993. http://www.sciencedirect.com/science/article/pii/S1352231007008217.

Kiselev, D., Bonacina, L., Wolf, J.-P., Nov 2011. Individual bioaerosol particle discrimination by multi-photon excited fluorescence. Opt. Express 19 (24), 24516–24521. http://www.opticsexpress.org/abstract.cfm?URI=oe-19-24-24516.

Kiselev, D., Bonacina, L., Wolf, J.-P., 2013. A flash-lamp based device for fluorescence detection and identification of individual pollen grains. Rev. Sci. Instrum. 84 (3), 033302. http://scitation.aip.org/content/aip/journal/rsi/84/3/10.1063/1.4793792.

Mie, G., 1908. Beiträge zur Optik trüber Medien, speziell kolloidaler Metallösungen. Ann. Phys. 330 (3), 377–445. http://dx.doi.org/10.1002/andp.19083300302.

Oteros, J., Galán, C., Alcázar, P., Domínguez-Vilches, E., 2013. Quality control in biomonitoring networks, Spanish aerobiology network. Sci. Total Environ. 443, 559–565. http://www.sciencedirect.com/science/article/pii/S0048969712014659.

Oteros, J., Pusch, G., Weichenmeier, I., Heimann, U., Möller, R., Röseler, S., Traidl-Hoffmann, C., Schmidt-Weber, C., Buters, J.T.M., 2015. Automatic and online pollen monitoring. Int. Arch. Allergy Immunol. 167 (3), 158–166. http://dx.doi.org/10.1159/000436968. http://www.karger.com/.

Pauling, A., Rotach, M., Gehrig, R., Clot, B., 2012. A method to derive vegetation distribution maps for pollen dispersion models using birch as an example. Int. J. Biometeorol. 56 (5), 949–958. http://dx.doi.org/10.1007/s00484-011-0505-7.

Perring, A.E., Schwarz, J.P., Baumgardner, D., Hernandez, M.T., Spracklen, D.V., Heald, C.L., Gao, R.S., Kok, G., McMeeking, G.R., McQuaid, J.B., Fahey, D.W., 2015. Airborne observations of regional variation in fluorescent aerosol across the United States. J. Geophys. Res. Atmos. 120 (3), 1153–1170. http://dx.doi.org/10.1002/2014JD022495, 2014JD022495.

Platt, J.C., 1999. Probabilistic outputs for support vector machines and comparisons to regularized likelihood methods. In: Advances in Large Margin Classifiers. MIT Press, pp. 61–74.

Pöschl, U., 2005. Atmospheric aerosols: composition, transformation, climate and health effects. Angew. Chem. Int. Ed. 44 (46), 7520–7540. http://dx.doi.org/10.1002/anie.200501122.

Puc, M., 2012. Influence of meteorological parameters and air pollution on hourly fluctuation of birch (Betula L.) and ash (Fraxinus L.) airborne pollen. Ann. Agric. Environ. Med. 19 (1), 660–665. http://dx.doi.org/10.1023/A%3A1007652220568.

Ring, J., Krämer, U., Schäfer, T., Behrent, H., 2001. Why are allergies increasing? Curr. Opin. Immunol. 13 (6), 701–708. http://www.sciencedirect.com/science/article/pii/S0952791501002825.

Sofiev, M., Siljamo, P., Ranta, H., Rantio-Lehtimäki, A., 2006. Towards numerical forecasting of long-range air transport of birch pollen: theoretical considerations and a feasibility study. Int. J. Biometeorol. 50 (6), 392–402.

Sutton, R.S., Barto, A.G., 1998. Reinforcement Learning: an Introduction, vol. 1. MIT press, Cambridge.

Tetko, I.V., Livingstone, D.J., Luik, A.I., 1995. Neural network studies. 1. Comparison of overfitting and overtraining. J. Chem. Inf. Comput. Sci. 35 (5), 826–833. http://dx.doi.org/10.1021/ci00027a006.

Vapnik, V.N., 1998. Statistical Learning Theory. Wiley Intersciences, New York.

Venables, W.N., Ripley, B.D., 2002. Modern Applied Statistics with S, fourth ed. Springer, New York. ISBN 0-387-95457-0. http://www.stats.ox.ac.uk/pub/MASS4.

Verein Deutscher Ingenieure, 2013. VDI 2119.

Vogel, H., Pauling, A., Vogel, B., 2008. Numerical simulation of birch pollen dispersion with an operational weather forecast system. Int. J. Biometeorol. 52 (8), 805–814. http://dx.doi.org/10.1007/s00484-008-0174-3.

Wüthrich, B., Schindler, C., Leuenberger, P., Ackermann-Liebrich, U., 1995. Prevalence of atopy and pollinosis in the adult population of Switzerland (Sapaldia study). Int. Arch. allergy Immunol. 106 (2), 149–156.

Zhou, Z., 2012. Ensemble Methods: Foundations and Algorithms. CRC Press, Taylor & Francis Group, Bocca Raton, FL.

Zink, K., Pauling, A., Rotach, M.W., Vogel, H., Kaufmann, P., Clot, B., 2013. Empol 1.0: a new parameterization of pollen emission in numerical weather prediction models. Geosci. Model Dev. 6 (6), 1961–1975. http://www.geosci-model-dev.net/6/1961/2013/.

Ziska, L., Knowlton, K., Rogers, C., Dalan, D., Tierney, N., Elder, M.A., Filley, W., Shropshire, J., Ford, L.B., Hedberg, C., et al., 2011. Recent warming by latitude associated with increased length of ragweed pollen season in central North America. Proc. Natl. Acad. Sci. 108 (10), 4248–4251.